

# Synthesis and characterization of mesoporous V-MCM-41 molecular sieves with good hydrothermal and thermal stability

Junqiang Xu, Wei Chu<sup>\*</sup>, Shizhong Luo

*Department of Chemical Engineering, Sichuan University, Yihuan Road, 24 South Section 1, Chengdu, Sichuan 610065, China*

Received 14 December 2005; received in revised form 28 March 2006; accepted 29 March 2006

Available online 5 June 2006

## Abstract

Stable V-MCM-41 mesoporous materials have been synthesized by hydrothermal method, using hexadecyl-trimethyl-ammonium bromide as template, and industrial  $\text{Na}_2\text{O}\cdot(3.3\text{--}3.5)\text{SiO}_2$  as the source of much cheaper silica instead of conventional expensive organic precursors. Several modern techniques like XRD,  $\text{N}_2$  adsorption, FT-IR, UV–vis and SEM have been utilized to characterize the framework structure and texture of the samples. The results of  $\text{N}_2$  adsorption and X-ray diffraction showed that the synthesized samples had a high ordered hexagonal structure, good hydrothermal stability and thermal stability. The selective oxidation of styrene using hydrogen peroxide as oxidant over V-MCM-41 samples showed a good catalytic performance of partial oxidation, the phenylacetic acid was the principal product (the selectivity value was 49.4%). Even after a thermal treatment at 900 °C in air for 12 h or a hydrothermal treatment in boiling water for 8 days, each of the two resultant materials could retain the ordered channels and a high BET surface area. UV–vis spectra provided strong evidences that most of vanadium ions were incorporated into the framework of siliceous MCM-41 sample.

© 2006 Elsevier B.V. All rights reserved.

**Keywords:** Mesoporous V-MCM-41; Hydrothermal stability; Thermal stability; Catalyst; Selective oxidation of styrene; Phenylacetic acid

## 1. Introduction

MCM-41 materials have become the most popular members of the M41s molecular sieve family since their discovery in 1992 and drawn considerable attention over the past decade [1,2]. MCM-41 materials with well-defined structure, uniform size distribution (1.5–10 nm), high internal surface area ( $\sim 1000 \text{ m}^2 \text{ g}^{-1}$ ), the cation-exchange and hydrocarbon-sorption capacities and high-density surface silanol sites, could be applied in many fields, such as catalysts or catalyst supports, chemical sorption, separation processes, environmental pollution control, electronic and optical materials [3,4].

Even though it is an attractive candidate, pure siliceous MCM-41 shows limited applications in organic transformations because neutral frame-structure of this material is lack of lacuna, acid sites and acidity. These lacuna, acid sites and acidities could give rise to the higher cation-exchange capacities and reactivity [5,6]. Modification of this material by the introduction of

various active metal incorporated into MCM-41 seemed to be a more interesting task for applications, owing to more acidic centers arising from the incorporated metals in the mesoporous materials. These materials have drawn more and more attention of academic and industrial researches in recent years [7–10].

Much recent attention has been directed towards their applications in catalysis. For practical application, a good catalyst needs not only a high initial catalytic activity, but also a good stability under process conditions. Therefore, the thermal stability and hydrothermal stability of these mesoporous materials become crucial factors in their potential applications. As a result of the hydrolysis of the Si–O–Si bonds in the presence of absorbed water, mesoporous silicate can lose its structure when it is exposed to high temperature or boiling water for a long period of time [11–13]. The collapse of the structure has limited the applications of MCM-41 materials, especially in the catalytic reactions involving the aqueous solution. In order to improve the thermal stability and hydrothermal stability of MCM-41 materials, several approaches have been exploited.

Introducing additive is an effective way for the stability improvement [14,15]. Yu et al. [13] reported that the stability of MCM-41 could be enhanced by the addition of a salt

<sup>\*</sup> Corresponding author. Tel.: +86 28 85403836; fax: +86 28 85405819.

E-mail addresses: [chuwei65@yahoo.com.cn](mailto:chuwei65@yahoo.com.cn), [chuwei65lille@yahoo.com](mailto:chuwei65lille@yahoo.com) (W. Chu).

to the gel mixture, due to the modulation of the electrostatic interaction between cationic surfactant micelles and silicate anions. But if the addition of salt was in unsuitable molar ratios, mesopore-structures would collapse and the pore size distribution became broad after a hydrothermal treatment.  $\text{La}_2\text{O}_3$  added into Al-MCM-41 improved its thermal stability at relatively lower temperature [16], but it was hardly beneficial to its high-temperature properties. Wang et al. [17] reported that the stability of MCM-41 was improved by introducing the building units of zeolite structure into the pore walls. Another route to improve the stability resorting to thicken the pore walls is altering synthesis conditions, such as in acidic or basic conditions, template agent, synthesis temperature and reaction time [18–20]. The combined effect of initial pH adjustment with direct addition of NaF into the reaction gel could lead to more hydrothermal stable MCM-41. It was reported recently that the inorganic silicate and organic surfactant precursors can self-organize to form ordered materials with nano-scale periodicities; this has created exciting avenues for the synthesis of mesoporous materials [21].

The aim of the current work was to synthesize and characterize the V-MCM-41 mesoporous molecular sieves and investigate the effects of different treatments on the stabilities of the samples with high ordered property. In this paper, the industrial inorganic silicate  $\text{Na}_2\text{O}\cdot(3.3\text{--}3.5)\text{SiO}_2$  was selected as a cheaper source of silica instead of expensive organic precursors, and the V-MCM-41 was prepared by direct hydrothermal synthesis. The framework structure, texture, thermal stability and hydrothermal stability of V-MCM-41 materials had been investigated; the X-ray diffraction (XRD),  $\text{N}_2$  adsorption/desorption and Fourier-transformed infrared (FT-IR) spectroscopy, diffuse reflectance UV–vis spectra, inductively coupled plasma technique (ICP), scanning electron microscopy (SEM) and differential thermogravimetric (DTG) analysis were utilized for the characterizations of catalysts. The selective oxidation of styrene was taken as a model reaction to investigate the potential catalytic applications of the V-MCM-41 sample of good stability.

## 2. Experimental

### 2.1. Precursor materials and synthesis of V-MCM-41 catalyst samples

Source of silica was  $\text{Na}_2\text{O}\cdot(3.3\text{--}3.5)\text{SiO}_2$  (Qiangwei Chemistry and Industry Co., Ltd., China). The vanadium source was  $\text{NH}_4\text{VO}_3$  (Shanghai Kechang Fine Chemical Plant, China). Quaternary ammonium surfactant was hexadecyl-trimethylammonium bromide (CTAB, Tianjin Bodi Chemicals, China).  $\text{H}_2\text{SO}_4$  (Shanghai Chemical Reagent Factory, China) was used for pH adjustment of the synthesis solution.

V-MCM-41 was synthesized as follows: pre-treatment: 6.045 g of  $\text{Na}_2\text{O}\cdot(3.3\text{--}3.5)\text{SiO}_2$  and 30 g deionized water was transferred into a Teflon-lined autoclave, and heated at  $110^\circ\text{C}$  for 12 h (h was utilized for a simplification of hours). The resultant solution was prepared for the further synthesis. Then, 5.467 g CTAB was diluted with 30 g deionized water under stirring at  $50^\circ\text{C}$ . After stirring for 0.5 h, the vanadium aqueous solution

(0.351 g  $\text{NH}_4\text{VO}_3$  dissolved in 40 g deionized water) was added dropwise to the template solution under vigorous stirring. Pre-treated sodium silicate solution was added dropwise to the above solution with stirring for another 0.5 h. The overall mixture composition was  $n(\text{Si}):n(\text{CTAB}):n(\text{V}):n(\text{H}_2\text{O}) = 1.0:0.2:0.04:100$ . Then 1 M  $\text{H}_2\text{SO}_4$  solution was added in order to reduce the pH value to  $\approx 9.5$ , and the stirring continued for another 2 h. The gel obtained was transferred into a Teflon-lined autoclave, and heated statically under autogenous pressure at  $110^\circ\text{C}$  for 48 h. The obtained materials were filtered, washed five times, dried at  $110^\circ\text{C}$  for 12 h, and then calcined at  $550^\circ\text{C}$  for 6 h.

### 2.2. Characterization of samples using different techniques

XRD patterns of the calcined samples were carried on a X-ray diffraction apparatus (Philips X'pert pro MPD) equipped with a graphite monochromator for Cu  $\text{K}\alpha$  (40 kV, 40 mA) radiation. Taking into account of large values of interplanar spacing in mesoporous molecular materials, the XRD patterns were recorded at low scattering angles between  $1.5^\circ$  and  $10^\circ$  ( $2\theta$ ).

The specific surface area, total pore volume and average pore diameter were measured by the  $\text{N}_2$  adsorption/desorption method with a Quantachrome Nova 1000e volumetric instrument at liquid nitrogen temperature. Samples were degassed at  $300^\circ\text{C}$  for 3 h prior to the analysis. The surface area was calculated by using the conventional BET method. The total pore volume was calculated from the amount of vapor adsorbed at a relative pressure ( $P/P_0$ ) close to unity. Pore size distributions were obtained using the BJH model and the desorption branch.

The FT-IR spectra of the calcined samples were measured using the KBr wafer technique in a Nicolet 170SX FTIR spectrometer (Nicolet, USA). The IR spectra were recorded in the range of  $4000\text{--}400\text{ cm}^{-1}$ .

UV–vis spectra of solid samples were recorded by the diffuse reflectance technique using Shimadzu UV-2401PC spectrophotometer in the range 200–600 nm, using  $\text{BaSO}_4$  as the reference.

The vanadium contents in the V-MCM-41 catalysts were analyzed by an inductively coupled plasma (ICP) technique using ICP-AES IRIS apparatus.

Thermogravimetric and differential thermogravimetric (TG-DTG) analysis were performed on a Perkin-Elmer TGA7 thermogravimetric analyzer. The sample was under an air atmosphere; the system temperature was risen from ambient to  $550^\circ\text{C}$  at a heating rate of  $10\text{ K min}^{-1}$ .

SEM images were obtained for the analysis of morphologies of surface particles of mesoporous samples using a JEOL JSM-5900LV scanning electron microscopy.

### 2.3. Hydrothermal treatment and thermal treatment of V-MCM-41 sample

The hydrothermal test: 1 g calcined V-MCM-41 sample was put into 100 mL boiled water and treated for different time (2, 4, 6, 8 and 10 days) in 100 mL of distilled water with a reflux condenser. After this treatment, the boiled sample was subsequently filtered and dried in an oven at  $110^\circ\text{C}$ .

The thermal test: 1 g calcined V-MCM-41 sample was calcined again at different temperature (600, 700, 800 and 900 °C) for 12 h in air.

#### 2.4. Catalytic evaluation in the selective oxidation of styrene

The selective oxidation of styrene was carried out in a round-bottom glass batch reactor fitted with a water-cooled condenser. In a typical reaction, 2.602 g styrene and 4.375 g acetone were added, then 0.250 g catalyst and 0.962 g hydrogen peroxide, the reactant mixture was heated with an oil bath at a temperature of 50 °C with magnetic stirring. After the reaction, the reaction mixture was cooled to room temperature, the catalyst was separated from the reaction mixture by centrifugation, and the reaction products were analyzed on a gas chromatograph (GC 112A) equipped with a flame ionization detector (FID) and a capillary column (cross-linked SE-30 gum, 0.33 mm × 30 m).

### 3. Results and discussion

#### 3.1. Texture analysis with $N_2$ -adsorption/desorption

Nitrogen physisorption is the technique to assess the textures of prepared MCM-41 mesoporous materials. A typical nitrogen sorption isotherm of V-MCM-41 at 77 K was shown in Fig. 1a (initial sample, 0 d), (0 d means 0 day, the initial sample, only calcined at 550 °C). The isotherm could be classified as a typical type Langmuir IV isotherm according to the IUPAC classification, which was typical of mesoporous materials. MCM-41 material contained a regular pore distribution with pores mainly in the mesopore size range where a characteristic capillary condensation occurred. A linear increase of absorbed volume at low pressures was followed by a steep increase in nitrogen uptake at a relative pressure  $P/P_0 = 0.3–0.4$ , which was due to capillary condensation inside the mesoporous at a characteristic relative pressure. The position of the inflection point was clearly related to the diameter of the mesopore, and the sharpness of this step indicated the uniformity of the mesopore size distribution [6,22]. The long plateau at higher relative pressures indicated that pore filling ranged from 0.40 to 1.0 ( $P/P_0$ ).

Hydrothermal stability was an important property of catalysts if one wishes to put those catalysts into usages of industrial heterogeneous catalysis. The mesoporous characteristic texture was shown after the samples were hydrothermally treated for 2, 4, 6, 8 and 10 days (Fig. 1a and b). After hydrothermal treatment for 2, 4 and 6 days, the isotherm of samples was belong to typical type mesoporous materials isotherm. Even 8-days hydrothermal treatment, the mesoporous structure of V-MCM-41 materials was retained. This result of our materials was somewhat better than that found by Marco [23], who found that MCM-41 was stable in boiling water only for 4 days at 100 °C. Our results were also better than those in a few references [24,25], which reported that the hydrothermal treatment time of samples with good hydrothermal stability did not surpass 6 days. The remaining ratio of surface area, pore volume and pore diameter were

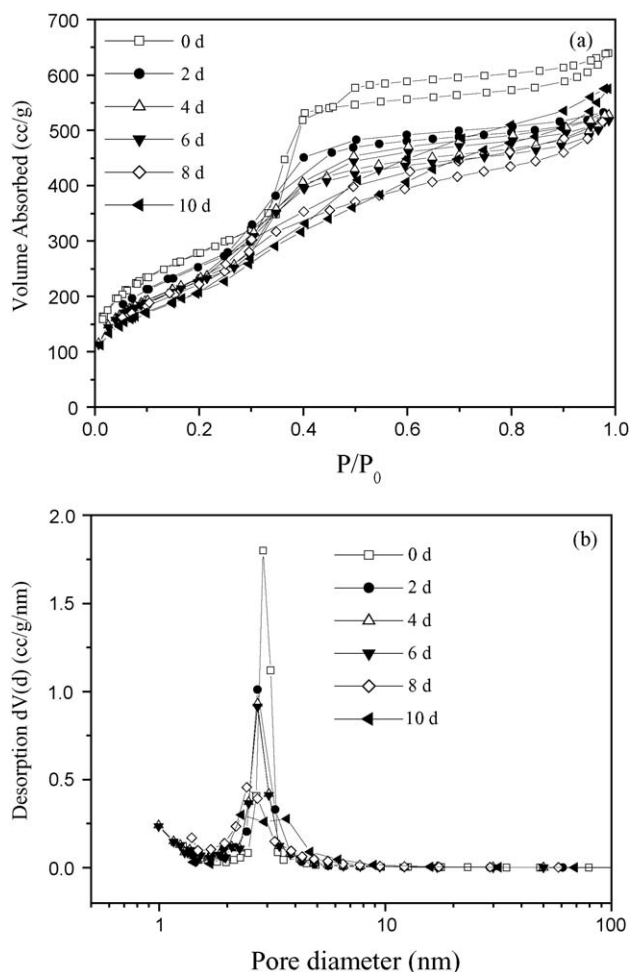


Fig. 1. (a) Nitrogen sorption isotherm at 77 K for six V-MCM-41 samples. (b) Resulting pore size distribution (BJH model, desorption branch) #V-MCM-41 synthesis condition:  $n(\text{Si}):n(\text{CTAB}):n(\text{V}):n(\text{H}_2\text{O}) = 1.0:0.2:0.04:100$ , pH  $\approx 9.5$ , crystallizing temperature at 110 °C for 48 h, calcined at 550 °C for 6 h (2 d means 2 days; 4, 6, 8, 10 d mean 4, 6, 8, 10 days).

84.3, 81.6, 91.9% for our prepared sample under hydrothermal treatment for 8 days in boiling water. Furthermore, after 10-days hydrothermal treatment, the mesoporous structure of this material was destroyed. However, the remaining ratio of surface area was 80.7%. For mesoporous materials, the capillary condensation was particularly interesting, which was related to the texture. Hydrothermal treatment had made the condensation step shift from the relative pressure  $P/P_0 = 0.3–0.4$  to  $P/P_0 = 0.2–0.5$ , which indicated that the pore diameter range shifted to a broader one and the BET surface became lower (Fig. 1b). The precursor of inorganic silicate [ $n(\text{Si}):n(\text{Na}) = 3.3–3.5$ ] introduced into the preparation system of mesopore-structure frameworks was responsible for the hydrothermal stability improvement [1,21]. The literature researches reported that the excess presence of sodium could destroy the hydrothermal stability of mesoporous materials. Our materials  $\text{Na}_2\text{O} \cdot (3.3–3.5)\text{SiO}_2$  in this text had less quantity  $\text{Na}^+$  comparing with that of conventional silicate of sodium  $\text{Na}_2\text{O} \cdot \text{SiO}_2$ , while the required Si quantity was kept the same. So, comparing the use of conventional silicate of sodium  $\text{Na}_2\text{O} \cdot \text{SiO}_2$  in which a large quantity of sodium could be harm-

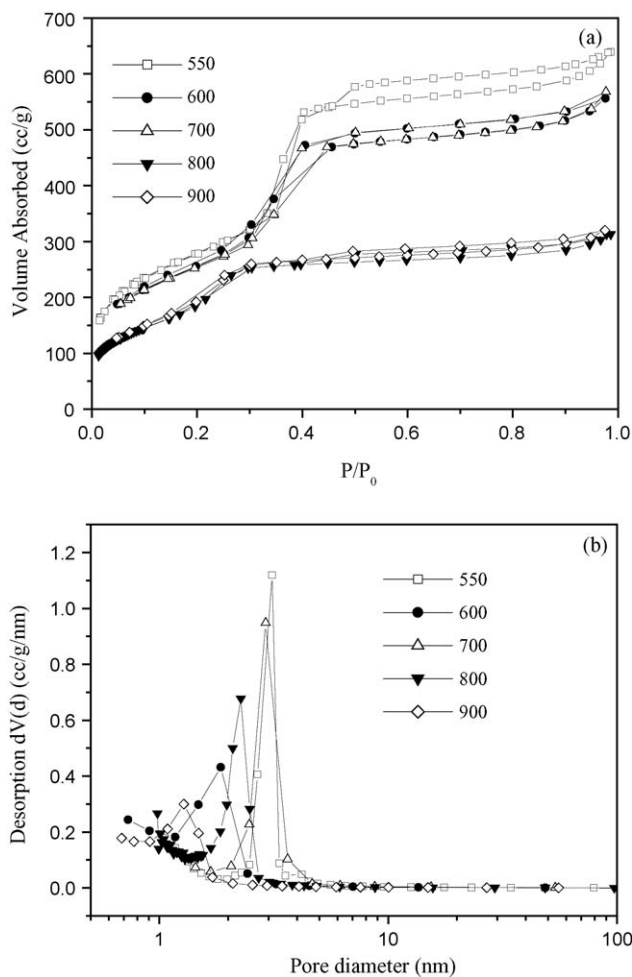


Fig. 2. (a) Nitrogen sorption isotherm at 77 K for the V-MCM-41 samples (calcined, respectively, at 550, 600, 700, 800, 900 °C in air atmosphere for 12 h). (b) Resulting pore size distribution (BJH model, desorption branch).

ful of the mesoporous structure, the sodium of less quantity in the raw materials  $\text{Na}_2\text{O} \cdot (3.3\text{--}3.5)\text{SiO}_2$  in this research, like the inorganic precursor of silica, did not affect the mesoporous structure during the hydrothermal synthesis. Then, using the filtration and several washing, the as-synthesized sample has only trace of sodium. The experiments of hydrothermal treatments indicated that the V-MCM-41 mesoporous material was of good hydrothermal stability. It could be said that this precursor of inorganic silicate with less sodium was helpful for the structure stability of the system.

The samples calcined at 550, 600, 700, 800 and 900 °C for 12 h in air were characterized by the  $\text{N}_2$  adsorption–desorption measurements (Fig. 2). The sharp reflection of samples isotherm took place shift a relative pressure  $p/p_0 = 0.3\text{--}0.4$  to  $p/p_0 = 0.2\text{--}0.3$ , which meant a typical capillary condensation within uniform pores and smaller pore diameter. After thermal treatment at 600 and 700 °C for 12 h, the isotherms hardly changed. This result was consistent with thermal treated at 800 and 900 °C for 12 h (Fig. 2a). The above results suggested that the materials were thermal stability in this temperature range. Pore diameter distribution became broader with increasing ther-

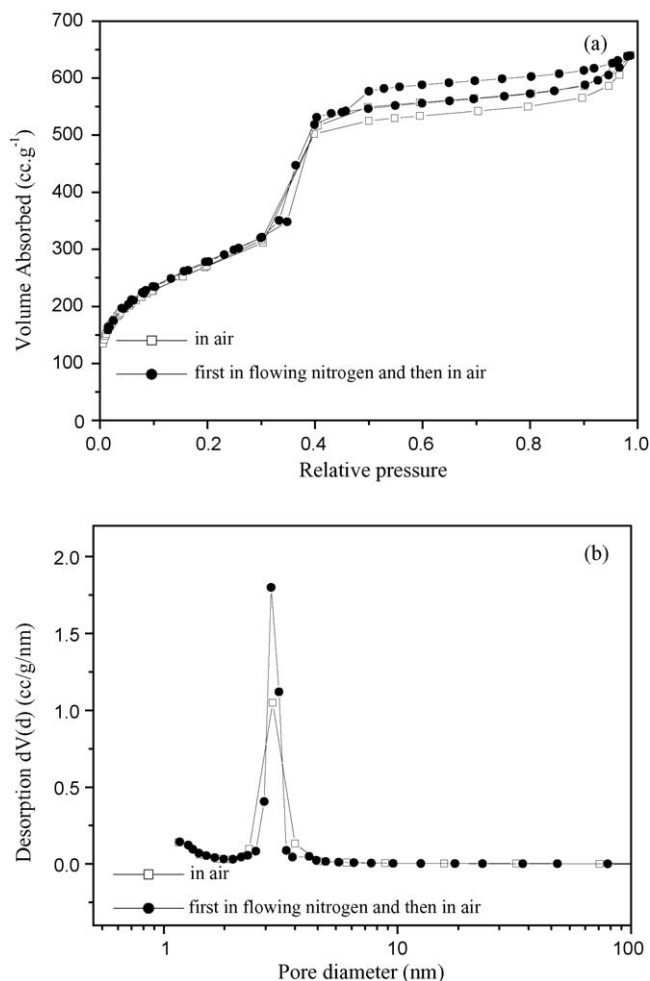


Fig. 3. (a) Nitrogen sorption isotherm at 77 K for two V-MCM-41 samples pretreated in different atmosphere and steps at 550 °C. (b) Resulting pore size distribution (BJH model, desorption branch).

mal treatment temperature, which indicated that the thermal treatment temperature destroyed slightly the materials (Fig. 2b). When the sample was thermally treated at 900 °C for 12 h, the mesopore-structure of this materials was retained. The remaining ratio of BET surface and pore diameter of the sample calcined in 900 °C for 12 h was 83.71% and 68.2%. Chen et al. [16] reported that the pore structure of MCM-41 collapsed when the calcination temperature was above 800 °C. The results of our experiments were better than those of a few previous researches [26–28], which reported that the samples were of good thermal stability.

No remarkable changes were observed for the isotherms of the V-MCM-41 sample at different calcinations atmosphere (Fig. 3). The isotherms of two samples showed a step increase at a certain relative pressure related to the specific pore diameter in the sample (Fig. 3a). This demonstrated that two samples had highly ordered regular pore structures. Fig. 3b showed also the pore size distributions, based on the  $\text{N}_2$  desorption isotherms for V-MCM-41 samples calcined at different atmosphere. The desorption isotherms indicated that the samples had very uniform pore size distributions.

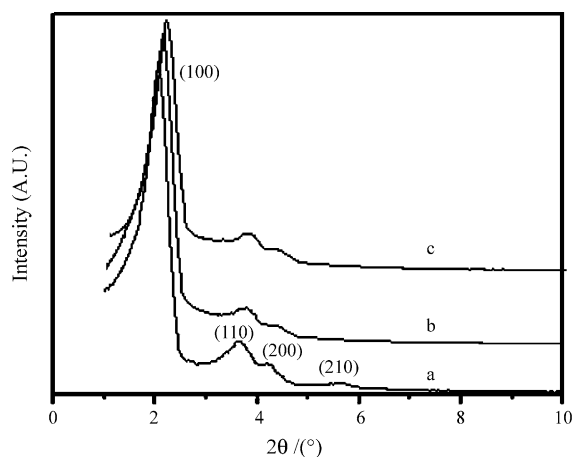


Fig. 4. X-ray diffraction data of hydrothermally treated V-MCM-41 samples, (a–c) sample after a hydrothermal treatment at boiling water, respectively, for 0, 4, 8 days, from the sample calcined at 550 °C.

### 3.2. Structure characterization using XRD technique

XRD is one of the most important techniques for characterizing the structure of crystalline or other ordered materials, which is capable of assessing the two-dimensional hexagonal structure. The crystallite phase of the vanadium-containing mesoporous molecular sieve was analyzed by X-ray powder diffraction. Fig. 4a showed the typical Bragg reflections of the hexagonal V-MCM-41 material as-synthesized at low angles, including a strong peak around 2.075° and three weak peaks at 3.605°, 4.175° and 5.645°, which could be indexed as (1 0 0), (1 1 0), (2 0 0) and (2 1 0) reflections of V-MCM-41, respectively, suggesting a perfect long-range order in this material [6]. Fig. 4(b and c) show the small-angle XRD patterns of hydrothermally treated samples for 4 and 8 days aging in boiling water on V-MCM-41 as-synthesized sample. Clearly, well-resolved (1 0 0), (1 1 0) and (2 0 0) diffraction peaks of V-MCM-41 were observed, which indicated that the mesopore-structure was kept almost totally even after 8 days aging in boiling water. The diffraction peaks became slightly broad and peak intensities decreased slightly with the augmentation of aging time in the boiling water, which indicated that the hydrothermal stability was weakened with the increasing of aging in the boiling water. This result was in agreement with that of N<sub>2</sub> adsorption. Typical values of structure and texture parameter were given in Table 1.

Table 1  
Structure and texture parameters of vanadium-containing mesoporous materials V-MCM-41 (a–d samples)

Sample	$d_{100}$ (nm)	$a_0$ (nm)	$\omega_t$ (nm)	$S_{\text{BET}}$ (m <sup>2</sup> g <sup>-1</sup> )	$V_p$ (cc g <sup>-1</sup> )	$D_p$ (nm)
a	4.279	4.94	0.996	1003	0.989	3.944
b	4.115	4.85	1.002	866	0.833	3.848
c	4.060	4.69	1.067	843	0.737	3.623
d	3.253	4.16	1.793	837	0.495	2.367

$d_{100}$  = XRD (1 0 0), interplanar spacing.  $a_0 = (2/\sqrt{3})d_{100}$ , unit cell parameter value;  $V_p$ , total pore volume at  $P/P_0 = 0.99$ ;  $D_p$ , average pore diameter;  $\omega_t = a_0 - D_p$ , frame wall thickness; (a–c) sample = the catalyst after the treatment of calcined sample in boiling water, respectively, for 0, 4 and 8 days. (d) Sample = the catalyst after a calcination in air at 900 °C for 12 h.

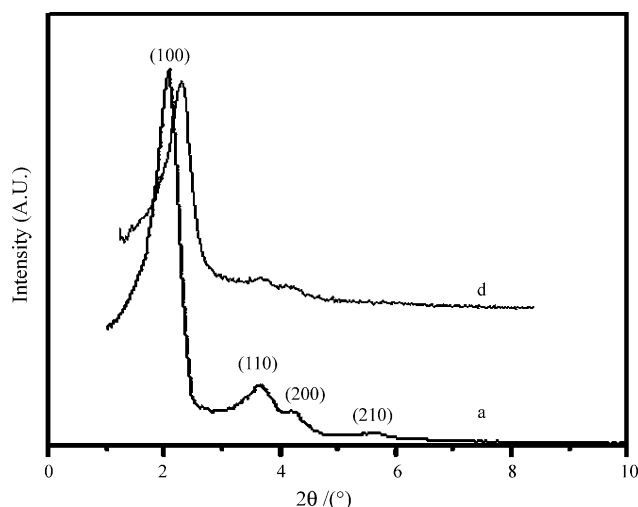


Fig. 5. X-ray diffraction patterns of thermally treated V-MCM-41 samples. (a and d) The samples calcined, respectively, at 550 and 900 °C in air.

The frame wall thickness increased after hydrothermal treatment or thermal treatment from Table 1.

Thermal stability was checked by subjecting the samples to temperatures up to 900 °C for 12 h. The XRD pattern (Fig. 5d) showed those peaks assigned to the hexagonal symmetry of mesoporous material. The resultant materials retained ordered channels even after thermal treatment at 900 °C for 12 h in air, which suggested that the V-MCM-41 sample was thermally stable. Consistent with the results from N<sub>2</sub> adsorption, it was shown that there was a high thermal stability.

### 3.3. Structure characterization using FT-IR technique

The presence of isolated surface silanols, hydrogen-bonded hydroxyl groups, and amorphous structures of the wall were evidenced from the FT-IR spectra of the calcined MCM-41 samples. The spectrum of V-MCM-41 sample remained closely as that of Si-MCM-41 (Fig. 6). The band at 480 and 800 cm<sup>-1</sup> could

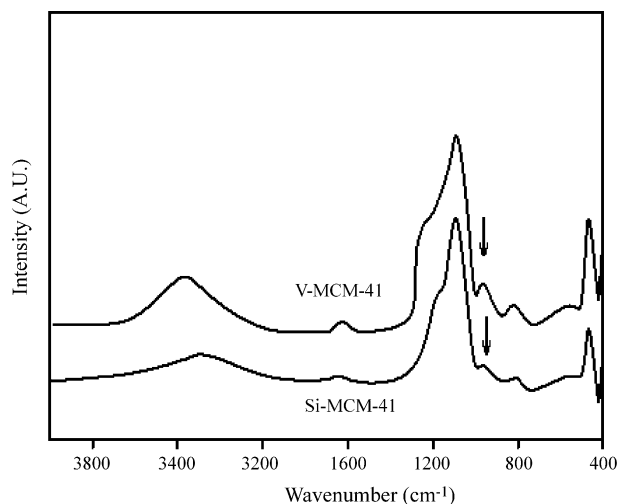


Fig. 6. FT-IR spectra of V-MCM-41 and Si-MCM-41 samples. Arrows marked the band at 960 cm<sup>-1</sup>.

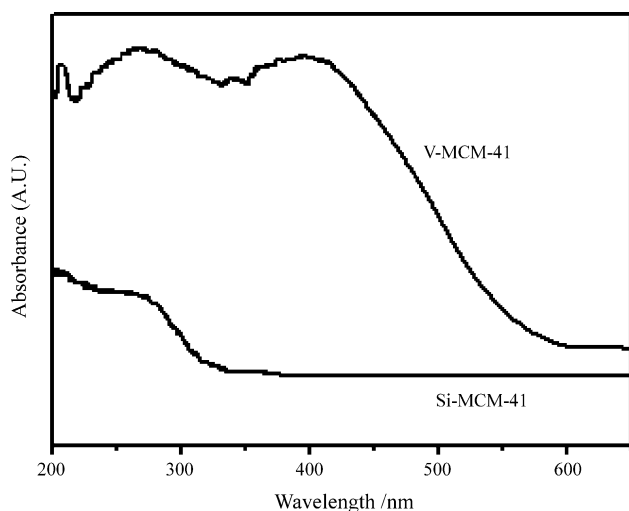


Fig. 7. UV-vis spectra of V-MCM-41 and Si-MCM-41 samples.

belong to the Si–O stretching vibrations and Si–O tetrahedron bonding vibration. A band at  $960\text{ cm}^{-1}$  was clearly visible in the spectra, which belonged to the framework V–O–Si stretching vibrations of molecular sieves V-MCM-41. This band was also observed in the MCM-41 sample, however, its intensity was much lower; in this case, it was due to the presence of silanol groups of the amorphous silica framework of MCM-41 sample. The band at  $960\text{ cm}^{-1}$  was attributed to Si–O–V band position, as these kinds of assignments were reported earlier for titanium-containing mesoporous materials [29,30]. So, the band in  $960\text{ cm}^{-1}$  could be taken as a proof for the incorporation of vanadium oxide in the framework of V-MCM-41 samples [1,31,32]. In the hydroxyl region ( $3600\text{--}3200\text{ cm}^{-1}$ ), a broad band was observed, assigned to the silanol groups inside the channels of Si-MCM-41. The FT-IR spectra were normally of amorphous wall characteristics, which indicated that the framework was made of the amorphous silica, although a perfect long-range order was present in this material.

#### 3.4. Structure characterization using diffuse reflectance UV-vis spectroscopy

Diffuse reflectance UV-vis spectra is a useful technique for obtaining information about the coordination environment and oxidation states of vanadium species in various molecular sieves. The different UV-vis Spectra of V-MCM-41 and Si-MCM-41 samples were shown in Fig. 7. The band observed at 220 nm was typical for siliceous materials, but new bands appeared in the 250–600 nm range after vanadium incorporation [31]. No absorption bands around 600–800 nm indicated the absence of d–d transitions. The band observed at 400 nm is usually assigned to the presence of extra framework vanadia species on the support surface. The intensity of the absorption band around 260 nm increased in V-MCM-41, due to the incorporation of V in the framework. Furthermore, direct information about the oxidation state and dispersion of vanadia species could be interpreted from the colour of the materials prepared [32]. After calcinations, the colour of as-synthesized Si-MCM-41 and vanadium-containing

mesoporous material V-MCM-41 were both white, after exposure to ambient conditions, the colour of V-MCM-41 material got yellowish and the Si-MCM-41 did not change, which shows a possible change in the coordination environment of the vanadium species. This colour change of V-MCM-41 indicated the possible alteration in the environment of the vanadia species by the coordination of water molecules from the atmosphere [33]. Moreover, after calcination, the vanadium species located on the surface could enhance the formation of V–O–V bonds, which are not evidenced from the IR measurements.

#### 3.5. Results of SEM analysis and of vanadium content analysis

The exact data of vanadium content of the mesoporous materials were measured by the ICP technique. The vanadium content of the V-MCM-41 was 15.0 mg/g. Scanning electron microscopy images was shown in Fig. 8a before the samples were hydrothermally and thermally treated tests. The micrographs revealed clearly that the resulting particles were almost perfectly spherical in shape. No agglomeration was visible. Small spherical particles of mesoporous silica V-MCM-41 sample with diameters of 90–250 nm were observed. The SEM analysis of samples calcined at 600, 700, 800 and 900 °C for 12 h in air was shown in Fig. 8(b–e). It was shown that the average diameter of observed particles increased slightly with the temperature rise of thermal treatment (calcinations), indicating a good thermal stability, which was consistent with the data of XRD and  $\text{N}_2$  adsorption.

#### 3.6. The decomposition properties characterized by TG-DTG method

The results of thermogravimetric analysis and differential thermogravimetric analysis for the MCM-41 and V-MCM-41 materials were depicted in Figs. 9 and 10. The TG/DTG spectra of the V-MCM-41 catalyst showed similar thermal phenomena as those of Si-MCM-41 material.

Four steps could be observed in the TG-DTG analysis. The first step of the sharp weight loss was observed from 30 to 110 °C, it was associated with the desorption of adsorbed water from the material, the percentage of weight loss was 3%. Two samples had almost same the percentage of weight loss.

The second part of the DTG curve, a further decomposition occurred at 110–280 °C, it was attributed to the thermal decomposition of silica precursor of silanol groups to the hexagonal mesoporous matrix. However, a detailed examination showed that the percentage of weight loss was smaller for V-MCM-41 catalyst (23.22%) than that of the corresponding Si-MCM-41 (29.22%). The third part, at 260–320 °C (V-MCM-41) and 280–350 °C (MCM-41), it was attributed to the decomposition and oxidation of the template. Nevertheless, the percentage of weight loss was larger for V-MCM-41 catalysts (11.08%) than that of the corresponding MCM-41 (5.99%) [17,34]. The last step in the DTG curve, the percentage of weight loss was 7.72% (V-MCM-41) and 5.01% (MCM-4) from 320 to 550 °C due to the condensation of residual silanols after the calcinations process. The differences signified that the interaction of the CTAB

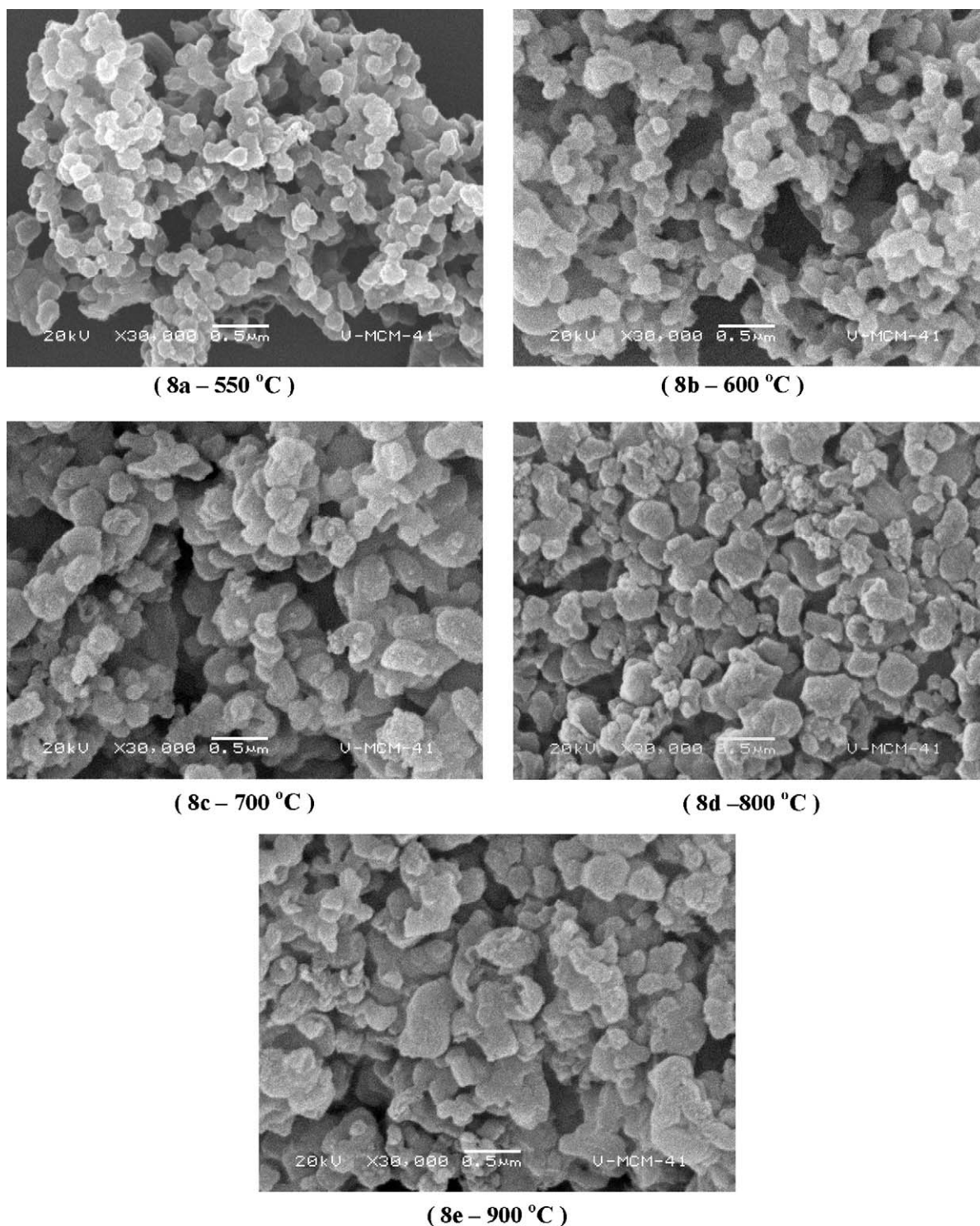


Fig. 8. SEM images of V-MCM-41 samples calcinated at different temperatures: (a) 550 °C; (b) 600 °C; (c) 700 °C; (d) 800 °C; (e) 900 °C.

with the silicate framework was weakened due to the effect of vanadium incorporating into the framework.

### 3.7. Catalytic performance in the selective oxidation of styrene

Results of catalytic evaluation on the selective oxidation of styrene using hydrogen peroxide over V-MCM-41 were

given in Table 2. In general, the selectivity of oxidation reaction was quite poor, with much formation of total oxidation product  $\text{CO}_2$ . To ensure a high selectivity of partial oxidation products, the new catalysts were investigated and developed, using  $\text{H}_2\text{O}_2$  as oxidant. In this research work, the styrene was an excessive reactant (its quantity was more than the stoichiometry amount comparing that of  $\text{H}_2\text{O}_2$ ), namely, acetone/styrene/oxidant (mol/mol) = 6/3/1. The  $\text{H}_2\text{O}_2$  was a limited

Table 2  
Effect of higher-temperature treatment of V-MCM-41 sample on the catalytic performance in the selective oxidation of styrene

Sample	$X(\text{H}_2\text{O}_2)$ (%)	Selectivity (%)			
		Benzaldehyde	Phenylacetaldehyde	Styrene epoxide	Phenylacetic acid
A	63.01	27.72	8.27	7.51	38.74
B	55.90	30.68	9.33	8.46	49.44
C	51.98	28.98	9.12	8.26	40.68
D	42.64	28.72	9.07	8.10	36.66
E	41.01	22.34	6.09	6.59	35.48
F	34.65	19.02	5.43	5.62	35.05

Reaction conditions: acetone/styrene/oxidant (mol/mol) = 6/3/1,  $T = 50^\circ\text{C}$ , catalyst amount = 250 mg, reaction time = 6 h. Sample A: calcined in air at  $550^\circ\text{C}$ ; sample B: calcined at  $550^\circ\text{C}$  in flowing nitrogen at first, then in air. Samples C–F: those hydrothermally treated at boiling water for 2, 4, 6 and 8 days, respectively, from the sample A.  $X(\text{H}_2\text{O}_2)$  (%): efficiency of oxygen usage, namely, the oxidant  $\text{H}_2\text{O}_2$  conversion.

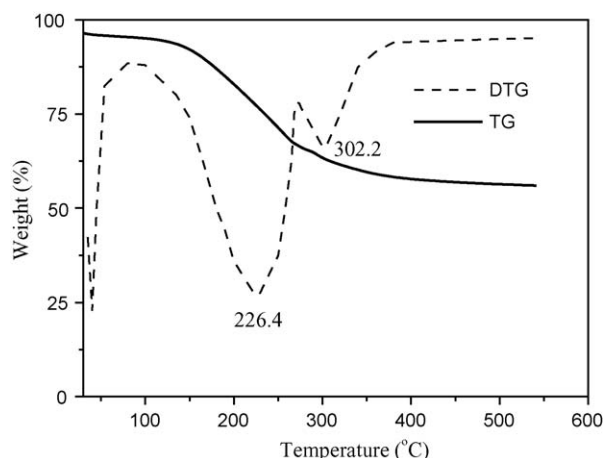


Fig. 9. TG-DTG curves of the MCM-41 sample as synthesized.

reactant. So, the activity calculations were based on the efficiency of oxygen usage, in other words, the conversion of  $\text{H}_2\text{O}_2$ .

The selective oxidation of styrene using hydrogen peroxide as oxidant over V-MCM-41 samples showed a good catalytic performance of partial oxidation, the phenylacetic acid was the principal most important product (the selectivity value was 49.4% for the sample (B) of V-MCM-41, which was calcined at  $550^\circ\text{C}$  in flowing nitrogen at first, then in air), at a  $\text{H}_2\text{O}_2$  conversion of 55.9%. The sample (A) of V-MCM-41, which was

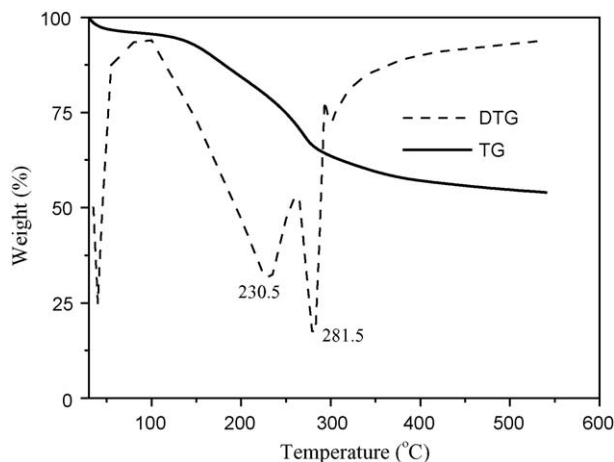


Fig. 10. TG-DTG curves of the V-MCM-41 sample as synthesized.

calcined only in air at  $550^\circ\text{C}$  gave a  $\text{H}_2\text{O}_2$  conversion of 63% with 38.7% selectivity in phenylacetic acid.

#### 4. Conclusions

Several V-MCM-41 mesoporous materials with different treatments were synthesized successfully, using cetyl-trimethylammonium bromide as template agent and an industrial inorganic silicate instead of expensive organic-silicate materials as a much cheaper silica source.  $\text{N}_2$  adsorption and X-ray diffraction results showed that the samples had a highly ordered hexagonal structure, good hydrothermal stability and thermal stability. FT-IR and UV-vis spectra provided strong evidences that most of vanadium ions were incorporated into the framework of siliceous MCM-41. The surface images of these mesoporous samples were analyzed using SEM technique. The TG and DTG analysis of MCM-41 and V-MCM-41 indicated the thermal decomposition property. The resultant materials retained ordered channels and high BET surface areas, even after a thermal treatment at  $900^\circ\text{C}$  for 12 h in air, or a hydrothermal treatment for 8 days in boiling water. The selective oxidation of styrene with hydrogen peroxide over V-MCM-41 catalysts showed that a good catalytic performance and a good selectivity of 49.4% in phenylacetic acid for sample (B) of V-MCM-41. The highly ordered mesoporous V-MCM-41 molecular sieves, with high thermal stability and hydrothermal stability, could be suitable for a variety of catalytic applications.

#### Acknowledgements

The authors are grateful to the National Natural Science Foundation of China for the support of this work (Project no. 20590363), also to the Innovation Fund of Sichuan University (Project no. 2005CF07). The authors acknowledge also the useful discussions with M.H. Chen, L.H. Huang, Z.M. Ci, L.N. Wang and J.Y. Hu of Sichuan University and the assistance of Z. Li of Analytic & Testing Center of Sichuan University and Prof. J.J. Zhu of Nanjing University.

#### References

- [1] K. Schumacher, C. du Fresne von Hohenesche, K.K. Unger, A. Du Chesne, U. Wiesner, H.W. Spiess, Adv. Mater. 11 (1999) 1194.



- [2] M. Selvaraj, P.K. Sinha, K. Lee, I. Ahn, A. Pandurangan, T.G. Lee, *Microporous Mesoporous Mater.* 78 (2005) 139.
- [3] J.Y. Ying, C.P. Mehnert, M.S. Wong, *Angew. Chem. Int. Ed.* 38 (1999) 56.
- [4] M. Mcnall, R.L. Laurence, W.C. Conner, *Microporous Mesoporous Mater.* 44 (2001) 709.
- [5] Russell F. Howe, *Appl. Catal. A Gen.* 271 (2004) 3.
- [6] M. Stöcker, *Microporous Mesoporous Mater.* 82 (2005) 257.
- [7] A. Sayari, Y. Yang, *J. Phys. Chem. B* 104 (2000) 4835.
- [8] D. Trong On, D. Giscard, C. Danumah, *Appl. Catal. A* 222 (2001) 299.
- [9] A. Sakthivel, S.K. Badamali, P. Selvam, *Microporous Mesoporous Mater.* 39 (2000) 457.
- [10] A. Sakthivel, J.S. Huang, H.W. Chen, *Adv. Funct. Mater.* 15 (2005) 253.
- [11] J.M. Kim, S. Jun, R. Ryoo, *J. Phys. Chem. B.* 103 (1999) 6200.
- [12] R. Mokaya, *J. Phys. Chem. B* 103 (1999) 10204.
- [13] J. Yu, J.L. Shi, H.R. Chen, *Microporous Mesoporous Mater.* 46 (2001) 153.
- [14] D. Trong On, S. Kaliaguine, *Angew. Chem. Int. Ed.* 41 (2002) 1040.
- [15] L. Huang, W. Guo, P. Deng, *J. Phys. Chem. B.* 104 (2000) 2817.
- [16] L.Y. Chen, S. Jaenicke, G.K. Chuah, *Microporous mater.* 12 (1997) 323.
- [17] S. Wang, T. Dou, Y.P. Li, *J. Solid State Chem.* 177 (2004) 4800.
- [18] Z. Zhang, Y. Han, L. Zhu, *Angew. Chem. Int. Ed.* 40 (2001) 1258.
- [19] W.J. Kim, J.C. Yoo, D.T. Hayhurst, *Microporous Mesoporous Mater.* 39 (2000) 177.
- [20] X. Chen, Y.C. Wang, *Ceram. Int.* 28 (2002) 541.
- [21] S.H. Tolbert, A. Firouzi, G.D. Stucky, et al., *Science* 278 (1997) 264.
- [22] Q. Cai, Z.S. Luo, W.Q. Pang, *Chem. Mater.* 13 (2001) 258.
- [23] M. Luechinger, L. Frunz, G.D. Pirngruber, R. Prins, *Microporous Mesoporous Mater.* 64 (2003) 203–211.
- [24] J.M. Kim, R. Ryoo, *Bull. Korea Chem. Soc.* 17 (1996) 66.
- [25] Q.H. Xia, K. Hidajat, S. Kawi, *Mater. Lett.* 42 (2000) 102.
- [26] P. Schacht, L. Norenã-Franco, J. Ancheyta, S. Ramírez, I. Hernández-Pérez, L.A. Garclá, *Catal. Today* 98 (2004) 115.
- [27] J. He, X. Duan, C.Y. Li, *Mater. Chem. Phys.* 71 (2001) 221.
- [28] Y.H. Yang, S.Y. Lim, C. Wang, *Microporous Mesoporous Mater.* 67 (2004) 245.
- [29] V. Pãrvulescu, C. Anastasescu1, B.L. Su, *J. Mol. Catal. A: Chem.* 198 (2003) 249.
- [30] F. Farzaneh, E. Zamanifar, D. Craig Williams, *J. Mol. Catal. A: Chem.* 218 (2004) 203.
- [31] B.S. Uphade, T. Akita, T. Nakamura, M. Haruta, *J. Catal.* 209 (2002) 331.
- [32] S. Shylesh, A.P. Singh, *J. Catal.* 228 (2004) 333.
- [33] Jino. George, S. Shylesh, P.A. Singh, *Appl. Catal. A: Gen.* 290 (2005) 148.
- [34] K. Fang, J. Ren, Y. Sun, *Mater. Chem. Phys.* 90 (2005) 16.